Article ID: 1006-8775(2018) 01-0015-14

INFLUENCE OF MODEL HORIZONTAL RESOLUTION ON THE INTENSITY AND STRUCTURE OF RAMMASUN

WANG Chen-xi (王晨稀), ZENG Zhi-hua (曾智华)
(Shanghai Typhoon Institute, CMA, Shanghai 200030 China)

Abstract: We use the WRF (V3.4) model as the experimental model and select three horizontal resolutions of 15, 9, and 3 km to research the influence of the model's horizontal resolution on the intensity and structure of the super-strong typhoon Rammasun (1409) in 2014. The results indicate that the horizontal resolution has a very large impact on the intensity and structure of Rammasun. The Rammasun intensity increases as the horizontal resolution increases. When the horizontal resolution increases from 9km to 3 km, the enhancement of intensity is more obvious, but the strongest intensity simulated by 3 km horizontal resolution is still weaker than the observed strongest intensity. Along with the increase of horizontal resolution, the horizontal scale of the Rammasun vortex decreases, and the vortex gradually contracts toward its center. The vortex structure changes from loose to compact and deep. The maximum wind radius, thickness of the eye wall, and outward inclination of the eye wall with height decrease, and the wind in the inner core region, updraft motion along the eye wall, and strength of the warm core become stronger. Additionally, the pressure gradient and temperature gradient of the eye wall region increase, and the vortex intensity becomes stronger. When the horizontal resolution increases from 9km to 3 km, the change in the Rammasun structure is much larger than the change when the horizontal resolution increases from 15km to 9 km. When the model does not employ the method of convection parameterization, the Rammasun intensity simulated with 3 km horizontal resolution is slightly weaker than the intensity simulated with 3 km horizontal resolution when the Kain-Fritsch (KF) convection parameterization scheme is adopted, while the intensity simulated with 9km horizontal resolution is much weaker than the intensity simulated with 9 km horizontal resolution when the KF scheme is adopted. The influence of the horizontal resolution on the intensity and structure of Rammasun is larger than the influence when the KF scheme is adopted.

Key words: horizontal resolution; Rammasun; intensity; structure
CLC number: P444 **Document code:** A
doi: 10.16555/j.1006-8775.2018.01.002

1 INTRODUCTION

For more than two decades, with the development of numerical forecast technology, the forecasting error of tropical cyclone (TC) track has decreased by nearly 50% (Duan et al.[1]; Xu et al.[2]; Qian et al.[3]), while the forecasting level of TC intensity has barely improved (Cangialosi and Franklin[4]). There are many factors that constrain the improvement of forecasting level for TC intensity, and insufficient model resolution is one of them that cannot be ignored.

The TC intensity forecasting is highly sensitive to the model resolution. Studies have found that for either an ideal TC (Hill and Lackmann [5]; Gopalakrishnan et al.[6]) or an actual TC (Braun and Tao [7]; Gentry and Lackmann [8]; Davis et al.[9]), under a normal situation, increasing the model horizontal resolution can enhance the forecasted TC intensity. When the horizontal resolution is 4 km, the intensity of the ideal TC reaches its strongest level, which approaches the maximum possible intensity (Hill and Lackmann[5]). The different horizontal resolution does not affect the development at the initial stage of ideal TC. At the mature stage of development, the vortex exhibits clear difference when simulated with different horizontal resolution (Gopalakrishnan et al.[6]). The forecasted TC intensity increases continuously as the model horizontal resolution increases because the higher the horizontal resolution is, the more physical processes the model can resolve, and some of these processes are very important to the intensity variation of TC (Gentry and Lackmann[8]). However, for different TC cases, there are also exceptions. The studies of Davis and Bosart [10] indicate that the intensity of Hurricane Diana (1984) at 9 km horizontal resolution is stronger than the intensity at 3 km horizontal resolution.

At present, it is commonly believed that when the horizontal resolution reaches 1–3 km, the model will be able to simulate and replay the variation process of TC intensity, especially the variation in the TC inner core.

Received 2017-02-07; **Revised** 2017-11-02; **Accepted** 2018-02-15
Foundation item: National Natural Foundation of China (41575108, 41275067, 41475082, 41475059); Special Scientific Research Fund of Meteorological Public Welfare of China (GYHY201506007)
Biography: WANG Chen-xi, M.S., Research Assistant, primarily undertaking research on tropical cyclones.
Corresponding author: ZENG Zhi-hua, e-mail: zengzh@typhoon.org.cn

In this situation, the model begins to exhibit some forecasting ability for TC intensity (Rogers[11]; Nguyen et al.[12]; Montgomery et al.[13]; Smith et al.[14]; Smith et al.[15]). However, the increase of model resolution is currently restricted by limited computational resources. As for the simulation and forecasting of TC intensity, it is still not clear at present what is the most reasonable, economical and applicable horizontal resolution. In addition, the existing studies on the influence of model horizontal resolution on TC intensity have mainly concentrated on ideal TC and Atlantic hurricanes, and there is no research on the TCs in the Northwest Pacific and South China Sea.

The No.9 TC Rammasun in 2014 is the strongest TC that has landed in China in the past 50 years. In this paper, we use the WRF (V3.4) model as the experimental model and select three horizontal resolutions of 15, 9, and 3 km to make experiments on Rammasun. Through these experiments, we investigate the influence of model horizontal resolution on the intensity and structure of Rammasun. This study will provide a basis for more effectively forecasting TC intensity.

2 EXPERIMENTAL MODEL, SCHEME AND DATA

The model used in the experiment is the WRF (V3.4) model, which is configured with two static, two-way nested domains. The coverage ranges of the outer and inner domain are approximately 5°S-45°N, 75°-150°E and 6°-31°N, 96°-133°E, respectively. We select three horizontal resolutions for the experiment, and the horizontal grid spacings of the outer/inner domains for the three experimental schemes are 45/15 km, 27/9 km, and 9/3 km, respectively. The following experimental results are all simulation results for the inner domains of different experimental schemes, namely, the simulation results for the horizontal resolution of 15, 9, and 3 km. Vertically, the model employs the terrain-following stationary pressure coordinate and there are 28 levels, with the pressure at the top level being 50 hPa.

The three experimental schemes use a consistent scheme of physical processes in the model, which is also the same in the inner and outer domains of the model. The convection parameterization scheme of the model is the Kain-Fritsch (KF) scheme. Whether or not the model uses the method of convection parameterization is not only related to the model horizontal resolution, but also to the scale of resolved convection. So the horizontal resolution with which the model can resolve the cumulus convection process without requiring parameterization is uncertain. It varies with the convection scale. It is usually believed that for the simulation of large-scale or middle-scale TC, when the horizontal resolution reaches 3-4 km, the model can avoid the use of the method of convection parameterization. In this paper, for consistency in the result comparison, we adopt the KF convection parameterization scheme for the horizontal grid spacings of 15, 9, and 3 km in the inner domain. Meanwhile, when the horizontal grid spacing in the inner domain is 9 km or 3 km, we also make the experiment without the method of convection parameterization. The schemes for other physical processes in the model include the YSU boundary parameterization scheme, WSM3 microphysics scheme, Dudhia shortwave radiation scheme, RRTM longwave radiation scheme, and Noah land surface scheme.

The data used in the experiment are the AVN initial field of the global spectral model with 1°×1° resolution. We initialize the data to form the model initial field and provide the lateral boundary for the model outer domain. The lateral boundary is updated every 6 h. We make the simulation experiment of Rammasun with different horizontal resolution, and the model integral time is 84 h. Corresponding to the horizontal resolutions of 45/15 km, 27/9 km, and 9/3 km, the step lengths of integral time are 150/50s, 90/30s, and 30/10s, respectively. During the model integral period, the sea surface temperature is changeless, set at 303K. The observation data used to verify the simulation results of Rammasun are from the TC best-track dataset compiled by the Shanghai Typhoon Institute, China Meteorological Administration (CMA-STI) (Ying et al.[16]).

3 OVERVIEW OF RAMMASUN

In 2014, TC Rammasun (1409) was generated over the ocean to the east of the Philippines in the afternoon of July 12. It intensified to a strong tropical storm in the morning of July 14 and then gradually approached the Philippines, intensifying to a typhoon during the night of that day. In the afternoon of July 15, it intensified to a strong typhoon and then landed along the coast in the middle of the Philippines. After landing, Rammasun turned in a northwest direction and intensified to become a super-strong typhoon. In the morning of July 16, it weakened to a strong typhoon and then further weakened to a typhoon later in the morning. It then entered the South China Sea and continued to move in a northwest direction. In the afternoon of July 17, it again intensified to a strong typhoon, and it intensified to a super-strong typhoon in the early morning of July 18. It reached its strongest intensity in the afternoon of July 18, when the maximum wind velocity near the center was 72m/s, and the lowest pressure at the center was 888hPa. It landed in Wenchang, Hainan, China at 15:30 Beijing Time (BJT) and then again in Xuwen, Guangdong at 19:30 BJT. After that, it entered the Beibu Gulf and weakened to a strong typhoon. At 07:10 BJT on July 19, it landed in Fangchenggang, Guangxi. After landing, Rammasun continued to move in a northwest direction and weakened to a typhoon in the

afternoon of July 19. After that, it entered the territory of Vietnam and weakened to a strong tropical storm during the night. Early in the morning of July 20, it weakened to a tropical storm and then dissipated to the north of Vietnam.

Rammasun landed on the coast of China three times, with a historically rare landing intensity. When it landed in Wenchang, Guangdong, the highest wind speed near the center was 70m/s, and the lowest pressure at the center was 890hPa. When it landed in Xuwen, Guangdong, the highest wind velocity near the center was 62m/s, and the lowest pressure at the center was 910hPa. They are both on the level of a super-strong typhoon. When it landed in Fangchenggang, Guangxi, the maximum wind velocity near the center was 50m/s, and the lowest pressure at the center was 945hPa, which is on the level of a strong typhoon. In particular, when it landed in Wenchang, Hainan, it is the strongest (in terms of the lowest pressure at the center) TC to have landed in China during the past 50 years.

In this paper, the simulation period of the Rammasun is from 08:00 BJT on July 16 to 20:00 BJT on July 19, a total of 84 h, when Rammasun left the Philippines to enter the South China Sea and landed three times on the coast of China before it eventually entered the territory of Vietnam. Its intensity undergoes the process of intensifying from typhoon to strong typhoon and super-strong typhoon and then weakening to strong typhoon, typhoon, strong tropical storm, and tropical storm.

4 EXPERIMENTAL RESULTS

4.1 *Track and intensity*

Figure 1 shows the Rammasun track simulated by the model over 84 h with three horizontal resolutions and the corresponding observed track when the KF convection parameterization scheme is adopted for the model inner domain. We can see from Fig.1 that the difference in the simulated tracks with the three horizontal resolutions is mainly in the moving velocity. When the horizontal resolution is 15 km, Rammasun moves fastest, and the motion is slowest when the horizontal resolution is 3 km. All three simulated tracks are very close to the observed track, only that when the horizontal resolution is 15 km, after landing, the simulated moving velocity is slightly faster than the observed, and when it is 3 km, it is slightly slower than the observed throughout the simulation process. When we do not adopt the method of convection parameterization in the inner domain, the track with 9 km and 3 km horizontal resolution (figure not shown) is similar to the track when the KF scheme is adopted. Table 1 gives the distance errors of the Rammasun simulated tracks with three horizontal resolutions. From the table, we can see that regardless of whether or not the method of convection parameterization is adopted, the track errors of 24 –84h for 12h interval are consistently within 100 km with the three horizontal resolutions, except for one value that is slightly larger than 100 km.

Generally, regardless of whether or not the method of convection parameterization is adopted in the model inner domain, the simulated tracks with the three horizontal resolutions are very close to the observed track. When the horizontal resolution is 9 km, the track is closest to the observed. Therefore, the variation in model horizontal resolution essentially does not affect the simulation of the Rammasun track significantly. This result is reasonable. The TC movement is mainly controlled by the environmental guiding airflow, and the forecasting of large-scale environmental field does not require high model resolution. The relatively accurate simulation of the Rammasun track with the three

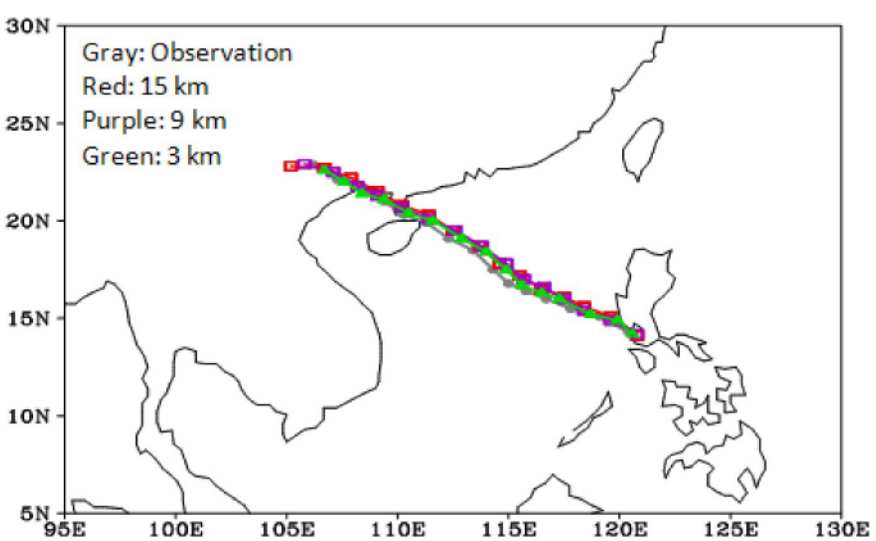

Figure 1. The observed track of Rammasun over 84h (from 08:00 BJT on July 16 to 20:00 BJT on July 19, with a time interval of 6 h) (gray) and the corresponding simulated tracks with three horizontal resolutions when we adopt the KF convection parameterization scheme in the model inner domain (red: 15 km, purple: 9 km, green: 3 km).

Table 1. Distance errors of the simulated tracks of Rammasun over 84 h (from 08:00 BJT on July 16 to 20:00 BJT on July 19) with three horizontal resolutions (unit: km)

Integral time (h)	KF convection parameterization scheme			Without convection parameterization	
	15 km	9 km	3 km	9 km	3 km
24	64.9	77.9	75.5	87.0	81.8
36	46.0	71.8	63.7	101.0	74.3
48	59.4	63.9	63.1	57.0	66.8
60	56.6	45.7	23.8	45.8	35.1
72	75.8	23.5	34.9	11.0	15.1
84	103.1	40.9	61.2	44.4	67.9

horizontal resolutions increases the reliability of the simulation results regarding the intensity and structure.

Figure 2 shows the evolution with time of lowest sea surface pressure of Rammasun observed and simulated with three horizontal resolutions, with the KF scheme and without adopting the method of convection parameterization in the model inner domain. Obviously, in contrast to the track simulation results, the Rammasun intensity is highly sensitive to the variation of horizontal resolution, and the simulated intensity increases with the increase of horizontal resolution. When we adopt the KF scheme in the inner domain, as we increase the horizontal resolution from 15 km to 9 km and then to 3 km, the simulated strongest intensity (in terms of the lowest sea surface pressure) of Rammasun changes from 922hPa to 920hPa and then to 913 hPa. We can see that when the horizontal resolution is increased to 3 km, the enhancement of the intensity is more obvious. Meanwhile, the time for the intensity to reach the strongest level is also the earliest for the 3 km horizontal resolution, earlier than the time for 15 km and 9 km by approximately 4 h, and the strongest intensity 913 hPa maintains for approximately 8h. Although the strongest intensity with the 3 km horizontal resolution reaches 913 hPa, it is still weaker than the observed strongest intensity (888 hPa). In addition, the time to reach the strongest intensity is earlier than the observed time. The time to reach the strongest intensity with the 15 km or 9 km horizontal resolution is relatively consistent with the observation, but the simulated strongest intensity is much weaker than the observed value.

When we do not adopt the method of convection parameterization in the inner domain, there is significant difference between the Rammasun intensity simulated with 3 km and 9 km horizontal resolution. Although the simulated intensity with the 3 km horizontal resolution is weaker than the intensity when the KF scheme is adopted, they are still relatively close. For the 9 km horizontal resolution, the simulated intensity is much weaker than the intensity when the KF scheme is adopted, and the influence of model horizontal resolution on intensity is very significant. Meanwhile, the time for the intensity to reach the strongest level with the 3 km horizontal resolution is later than the time when the KF scheme is adopted, but it is relatively consistent with the observed time. For the 9 km horizontal resolution, the time to reach the strongest level is later than the time when the KF scheme is adopted and is also later than the observed time. Here, we can also see that the 9 km horizontal resolution cannot very well resolve the convection process of Rammasun, and it still needs to take advantage of the parameterization method. This result also indicates the significance of convection process in the variation of Rammasun intensity.

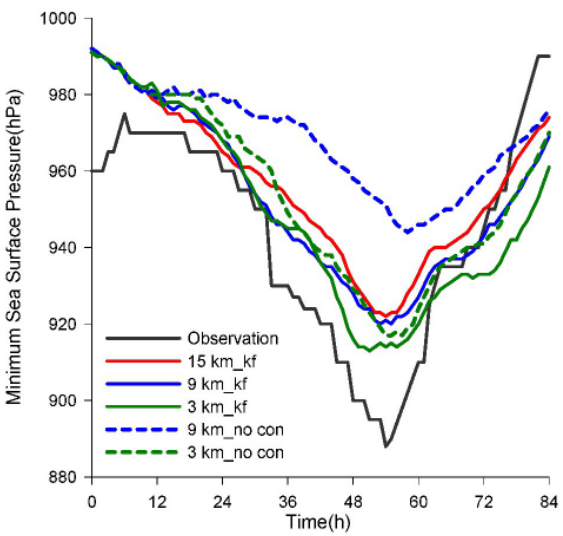

Figure 2. Evolution of lowest sea surface pressure of Rammasun with time (from 08:00 BJT on July 16 to 20:00 BJT on July 19) from the observation and simulation with three horizontal resolutions (black solid line: observation, red solid line: 15km_KF scheme, blue solid line: 9km_KF scheme, green solid line: 3 km_KF scheme, blue dashed line: 9 km_non-convection scheme, green dashed line: 3 km_non-convection scheme).

The following sections 4.2-4.4 provide the simulation results when the KF convection parameterization scheme is adopted in the model inner domain, while the simulation results without adopting the method of convection parameterization in the inner domain are given in section 4.5.

4.2 *Evolution of inner core structure*

The variation of TC intensity is closely related to the variation of TC structure. We compare the structure

and variation of Rammasun vortex simulated with three horizontal resolutions.

Figure 3 shows the evolution of axisymmetric tangential wind at 10m-height with time for Rammasun simulated with three horizontal resolutions. We can see from the figure that for the horizontal resolution of 15, 9, and 3 km, the maximum wind radius of Rammasun gradually decreases as the maximum wind increases. As the maximum wind reaches the maximum, the maximum wind radius reaches the minimum when the Rammasun intensity reaches its strongest level (Fig.2). After that, the maximum wind radius gradually increases as the maximum wind decreases. The variation of strong wind radius is opposite to the variation of maximum wind radius. The strong wind regions of ⩾20m/s, 30m/s, and others all first gradually expand outward and their radii gradually increase. After the maximum wind reaches the maximum, the strong wind regions gradually contract inward and their radii gradually decrease.

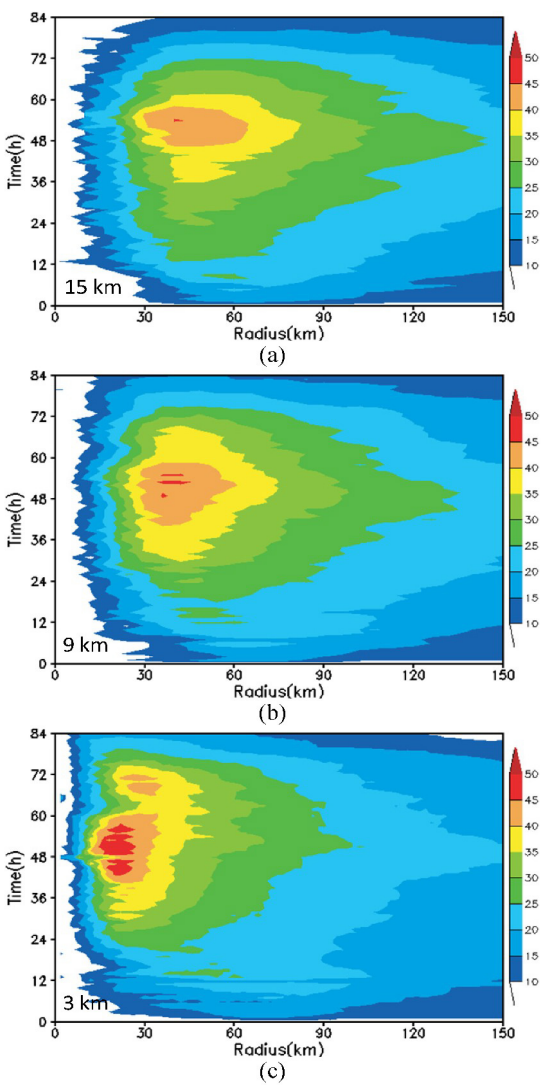

Figure 3. Temporal evolution of axisymmetric tangential wind at 10m-height (from 08:00 BJT on July 16 to 20:00 BJT on July 19) for Rammasun simulated with three horizontal resolutions (unit: m/s; a: 15 km, b: 9 km, c: 3 km).

Although the evolution process of Rammasun vortex simulated with three horizontal resolutions is analogous, the difference in vortexes with three horizontal resolutions is also obvious. We can see from Fig.3 that as the horizontal resolution increases, the maximum wind radius and strong wind radius all gradually decrease, and the thickness of eye wall decreases and the wind in the eye wall region becomes stronger. This change is more obvious when the horizontal resolution increases from 9 km to 3 km. For example, at approximately 54 h, the maximum wind radius decreases from about 40 km to only about 20 km.

To better understand the influence of horizontal resolution on the Rammasun vortex structure, we give Fig.4 which shows the horizontal wind at 10m-height at 48h (08:00 BJT on July 18) for Rammasun simulated with three horizontal resolutions. From Fig.4a-4c, we can see that the vortex horizontal scale simulated with 3 km horizontal resolution is much smaller than the scale with 9 km horizontal resolution. When the horizontal resolution changes from 9 km to 3 km, the region with wind speed ≥ 30m/s decreases by approximately 70%. The wind in the inner core region with 3 km horizontal resolution is much stronger than the wind with 9 km horizontal resolution. The vortex horizontal scale and wind in the inner core region with 9 km horizontal resolution show relatively small difference from those with 15 km horizontal resolution. We can also see from this figure that, no matter with 15, 9 or 3 km horizontal resolution, the distribution of horizontal wind is asymmetric, and the wind on the right of the moving direction of Rammasun is obviously larger than the wind on the left.

From Fig.4d-4f, we can more clearly see that the Rammasun vortex structure is very tight with 3 km horizontal resolution. From the vortex periphery inward, the horizontal wind increases rapidly and reaches the maximum ⩾60m/s in the eye wall region. From the eye wall region further inward to the eye region, the horizontal wind decreases abruptly, making the radial gradient of horizontal wind extremely large. Comparatively speaking, when the horizontal resolution is 9 km and 15 km, the vortex structure is relatively loose, and the horizontal wind and its gradient in the inner core region are both much smaller than those with 3 km horizontal resolution. Although there is difference between the vortex structure simulated with 9 km and 15 km horizontal resolution, it is much smaller than the difference between 9 km and 3 km resolution.

The distribution of relative vorticity at 10m-height at 48h (08:00 BJT on July 18) for Rammasun simulated with three horizontal resolutions (Fig.5) is similar to that of horizontal wind (Fig.4d-4f). The results in Fig.5 further indicate the influence of the variation of horizontal resolution on vortex structure. As the horizontal resolution increases, especially when it

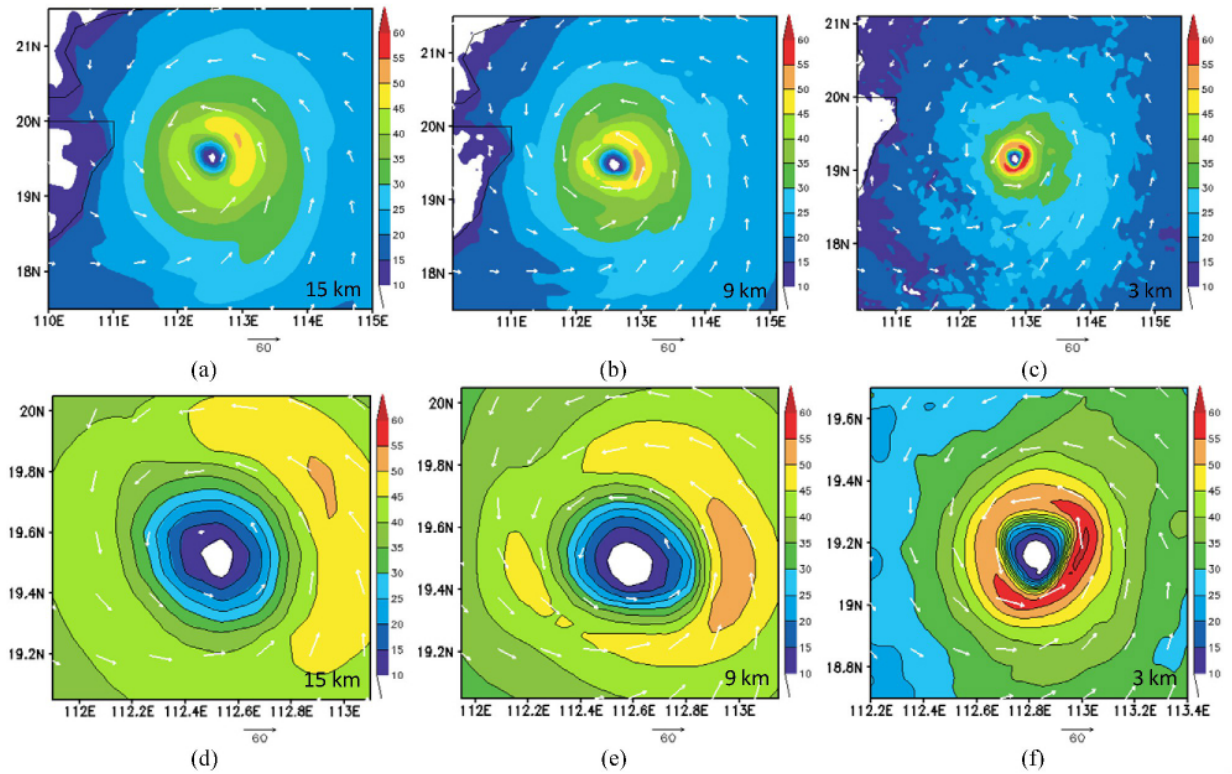

Figure 4. Horizontal wind (a-c) and horizontal wind in the zoomed-in inner core region (d-f) at 10m-height at 48h (08:00 BJT on July 18) for Rammasun simulated with three horizontal resolutions (unit: m/s; a, d: 15 km; b, e: 9 km; c, f: 3 km)

increases from 9 km to 3 km, the simulated vortex structure changes from loose to very compact, and the vortex horizontal scale decreases considerably and the intensity increases significantly. The largest relative vorticity, which is located in the southeast quadrant, is less than $3/10^3 \cdot s$ when the horizontal resolution is 15 km. It increases to near $5/10^3 \cdot s$ with 9 km horizontal resolution and increases to above $10/10^3 \cdot s$ with 3 km horizontal resolution.

In the studies of Atlantic hurricanes, Yau et al.[17] and Davis et al.[18] have noted the influence of model horizontal resolution on the inner core structure of TC. Yau et al.[17] found that compared with the simulation results with 6 km horizontal resolution, the eye wall of Andrew (1992) with 2 km horizontal resolution is more compact, and its width decreases by half, while the maximum wind radius decreases by 10-20 km. The simulation results of Rammasun in this paper are consistent with the results of Yau et al.[17] and Davis et al.[18]. The higher the horizontal resolution, the smaller the horizontal scale of vortex and the more compact the vortex structure, and the smaller the thickness of eye wall and the maximum wind radius. The reduction of the eye wall thickness makes the pressure gradient force in the eye wall region increase, which in turn makes the wind in the eye wall region increase. Therefore the vortex intensity is stronger. This change is much greater when the horizontal resolution increases from 9 km to 3 km than the change when it increases from 15 km to 9 km.

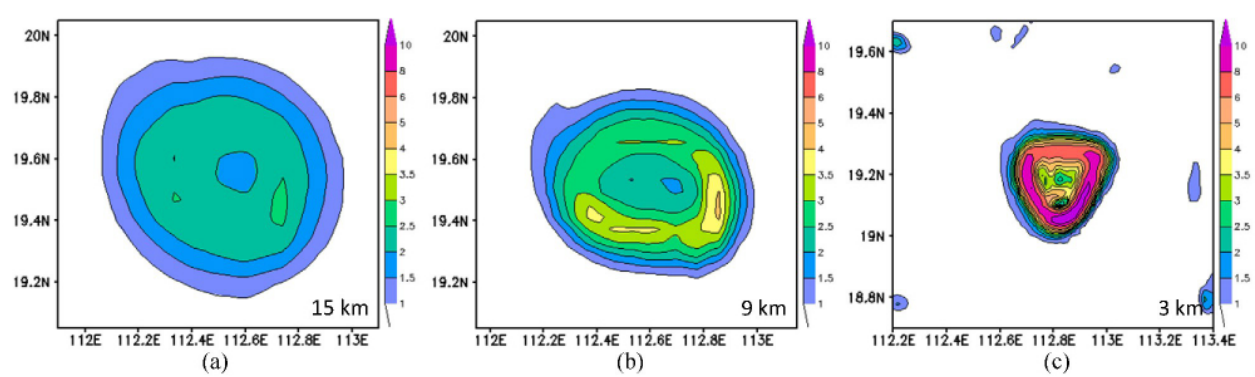

Figure 5. Relative vorticity at 10m-height at 48h (08:00 BJT on July 18) for Rammasun simulated with three horizontal resolutions (unit: $1/10^3 \cdot s$; a: 15 km, b: 9 km, c: 3 km).

4.3 *Structure of warm core and its variation*

The variation of TC intensity is accompanied with that of the high-level warm core. We compare the structure and variation of Rammasun warm core simulated with three horizontal resolutions.

Figure 6 shows the *x-z* cross-section of temperature anomaly and specific humidity across the Rammasun center at 48 h (08:00 BJT on July 18) simulated with three horizontal resolutions. We can see from the figure that when the horizontal resolution changes, the change of the Rammasun warm core structure is consistent with that of its vortex structure. As the horizontal resolution increases, the warm region located at the middle and high levels of Rammasun gradually contracts inward and becomes narrow, and the strength of warm core gradually increases. As the horizontal resolution changes from 15 km to 9 km and then to 3 km, the largest temperature anomaly increases from 12K to more than 13K and further to above 15K, and the height of the largest temperature anomaly declines slightly. We can also see from the figure that the humidity in the eye wall region is higher than the humidity in eye region, and their difference increases as the horizontal resolution increases.

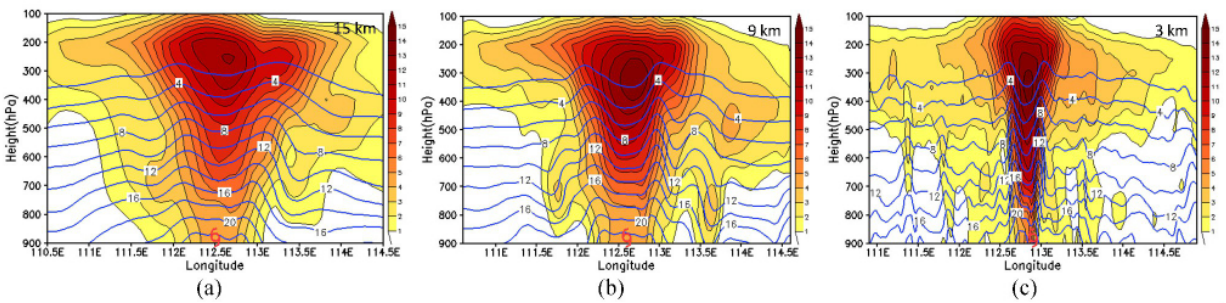

Figure 6. The *x-z* cross-section of temperature anomaly (color shaded, unit: K) and specific humidity (contour, unit: g/kg) across Rammasun center at 48 h (08:00 BJT on July 18) simulated with three horizontal resolutions (a: 15 km, b: 9 km, c: 3 km; the typhoon symbol indicates the Rammasun position).

Consequently, when the horizontal resolution increases, the vortex structure changes from loose to compact. The strength of warm core increases as the eye region decreases and the thickness of eye wall narrows, causing the eye region to become warmer and drier. The intensification of warm core and the narrowing of the eye wall thickness cause the temperature gradient and humidity in the eye wall region to increase. From Fig.6, we can also observe that from low levels to high levels, the eye wall is gradually inclined outward, and the inclination decreases as the horizontal resolution increases.

By examining the Rammasun's temporal evolution of axisymmetric potential temperature at 400hPa-height (Fig.7) and that of axisymmetric largest temperature anomaly (Fig.8), both simulated with three horizontal resolutions, we can understand the variation of warm core with time for different horizontal resolution.

From Fig.7, we can see that regardless of whether the horizontal resolution is high or low, the average potential temperature at 400hPa-height first gradually increases and then gradually decreases after reaching the maximum between 48h and 60h, which is consistent with the variation of vortex intensity (Fig.3). The higher the horizontal resolution, the faster and the higher the rise of potential temperature after 24 h. For 3 km horizontal resolution, the time for potential temperature to reach 346K is the earliest in the three horizontal resolutions. It continues to rise and reaches above 356K near 48h and remains at this value until approximately 58h. For 9 km horizontal resolution, the time to reach 346K is slightly later than the time for 3 km horizontal resolution, and although its maximum reaches 356K, it only remains at this value for approximately 2 h. For 15 km horizontal resolution, the time to reach 246K is the latest, and its maximum is less than 356K. As the horizontal resolution increases, the region with high potential temperature gradually contracts inward, and

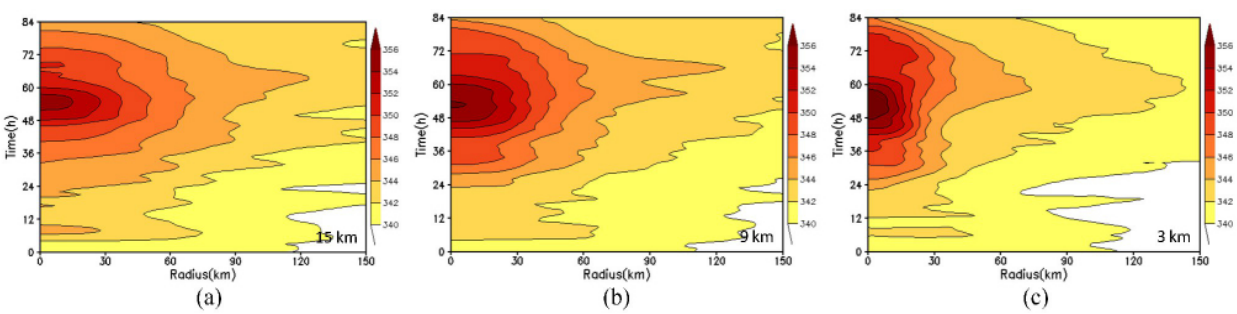

Figure 7. Temporal evolution of axisymmetric potential temperature at 400hPa-height (from 08:00 BJT on July 16 to 20:00 BJT on July 19) for Rammasun simulated with three horizontal resolutions (unit: K; a: 15 km, b: 9 km, c: 3 km)

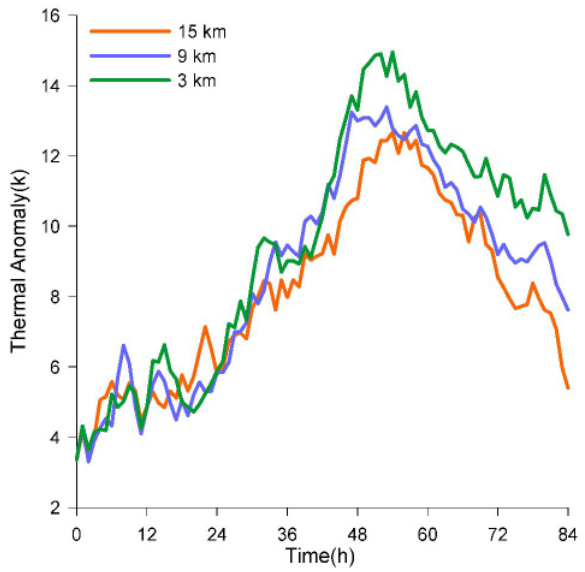

Figure 8. Temporal evolution of axisymmetric maximum temperature anomaly (from 08:00 BJT on July 16 to 20:00 BJT on July 19) for Rammasun simulated with three horizontal resolutions (orange: 15 km, blue: 9 km, green: 3 km).

the potential temperature gradient increases.

Figure 8 reflects the variation of the strength of Rammasun warm core with time for the three horizontal resolutions. We can see from the figure that, same as the results in Fig.7, although the strength of warm core with different horizontal resolution is different, their variation trend is the same. Difference of the warm core strength with different horizontal resolution is more obvious after 24 h. After approximately 30h, the strength of warm core with 15 km horizontal resolution is weaker than the strength with 9 km and 3 km horizontal resolution, and after approximately 42 h, the strength of warm core with 9 km horizontal resolution is weaker than the strength with 3 km horizontal resolution. This result is exactly the same as the result of Rammasun intensity simulated with three horizontal resolutions (Fig.2). Therefore, the variation of Rammasun warm core is consistent with the variation of Rammasun intensity, and the Rammasun intensity and the strength of Rammasun warm core both increase as the horizontal resolution increases.

From Fig.10 in section 4.4, we can see that the higher the horizontal resolution, the stronger the updraft motion along the eye wall. The stronger updraft motion transports more heat and water vapor from boundary layer to high levels. More heat transportation and the heat released by more condensation of water vapor result in a stronger warm core, and more water vapor transportation also increases the humidity in the eye wall region. With higher horizontal resolution, stronger updraft motion decreases the surface pressure while transporting more water vapor and heat, and then the surface wind becomes stronger. In addition, the higher the horizontal resolution, the larger the temperature gradient in the eye wall region, which further reinforces the vortex and its circulation. All of these factors increase the Rammasun intensity.

4.4 *Axisymmetric structure and vertical wind shear*

TC is a kind of deep weather system, and it can extend upward from the ground surface to 200hPa-height or even higher altitude. We further compare the vertical structure of Rammasun simulated with three horizontal resolutions. Here, we give the axisymmetric 12-hourly (from 02:00 to14:00 BJT, July 18) time-averaged radius-height cross-section of tangential wind (Fig.9), vertical upward wind (Fig.10), equivalent potential temperature (Fig.11) and potential vorticity (Fig.12) of Rammasun simulated with three horizontal resolutions. During 02:00-14:00 BJT on July 18, the Rammasun intensity rapidly increased to the strongest level in its lifetime (Fig.2), and the 12-hourly time-averaged results of 02:00-14:00 BJT on July 18 reflect the average vertical structures of Rammasun during the stage of rapid enhancement.

From the radius-height cross-section of tangential wind (Fig.9), we can see that regardless of whether the horizontal resolution is high or low, the average tangential wind decreases with height. As the horizontal resolution increases, the strong wind region extends upward to higher altitude. For example, for 15 km horizontal resolution, the region with the average tangential wind greater than 55m/s extends to approximately 750hPa-height, while for 9 km and 3 km horizontal resolution, it extends to approximately 650hPa- and 500hPa-height, respectively. For the height

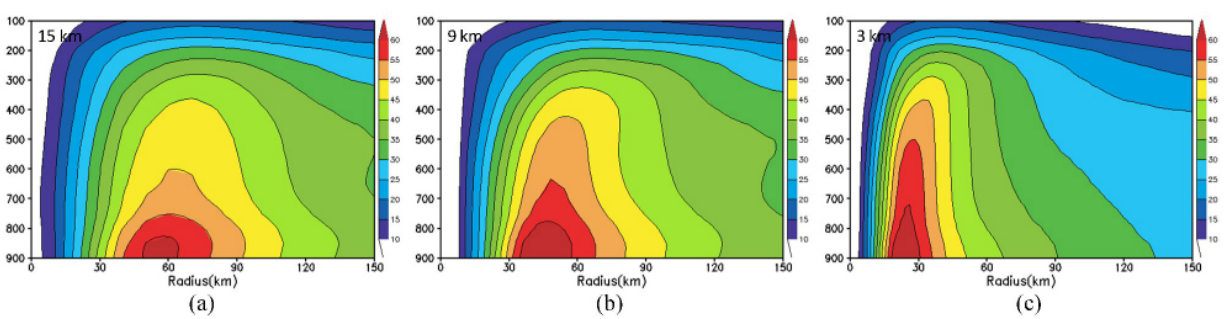

Figure 9. Axisymmetric 12-hourly (02:00-14:00 BJT, July 18) time-averaged radius-height cross-section of tangential wind of Rammasun simulated with three horizontal resolutions (unit: m/s; a: 15 km, b: 9 km, c: 3 km)

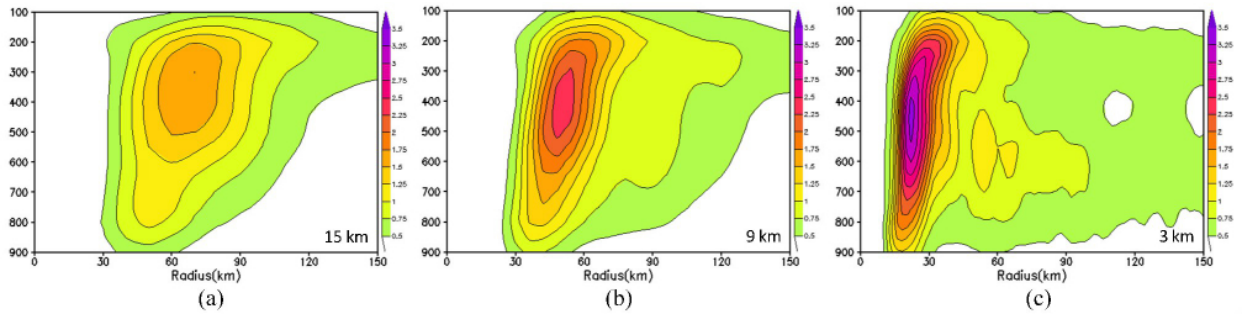

Figure 10. Axisymmetric 12-hourly (02:00-14:00 BJT, July 18) time-averaged radius-height cross-section of vertical upward wind of Rammasun simulated with three horizontal resolutions (unit: m/s; a: 15 km, b: 9 km, c: 3 km).

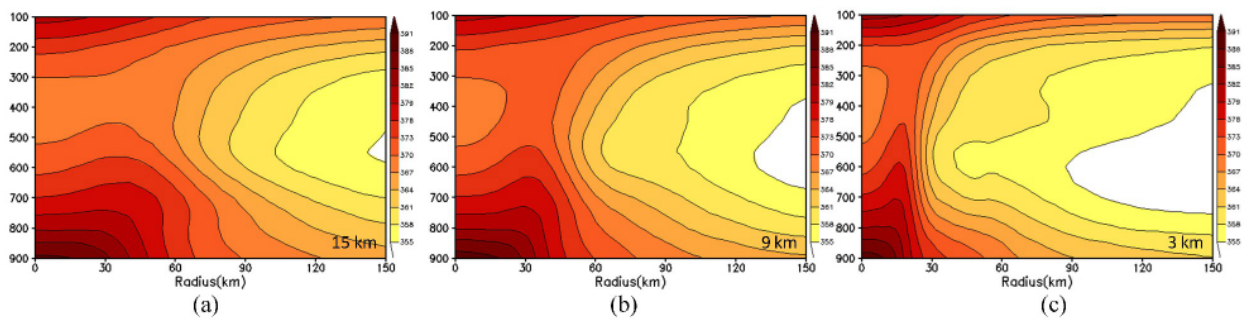

Figure 11. Axisymmetric 12-hourly (02:00-14:00 BJT, July 18) time-averaged radius-height cross-section of equivalent potential temperature of Rammasun simulated with three horizontal resolutions (unit: K; a: 15 km, b: 9 km, c: 3 km).

the region with relatively weak wind reaches, there is no considerable difference among the three horizontal resolutions. For both the strong wind region and the weak wind region, the region's radial width decreases as the horizontal resolution increases. When the horizontal resolution increases from 15 km to 9 km and further to 3 km, the radial width of the region with average tangential wind greater than 45 m/s at 900 hPa-height decreases from approximately 75 km to approximately 70 km and then to approximately 35 km. In addition, the maximum wind radius and the thickness of eye wall also decrease as the horizontal resolution increases. Overall, as the horizontal resolution increases, the vortex structure becomes more compact and deeper. When the horizontal resolution increases from 9 km to 3 km, this change is more obvious.

From Fig.9, we can also see that regardless of whether the horizontal resolution is high or low, the vertical profile of maximum wind radius is inclined outward with height, and the inclination is more obvious at the middle and high levels. As the horizontal resolution increases, the inclination of the vertical profile gradually declines. Stern and Nolan[19] observed a linear relationship between the outward inclination of maximum wind radius with height and the scale of maximum wind radius. The larger the maximum wind radius, the larger the outward inclination with height. The results in Fig.9 are consistent with the findings of S tern and Nolan[19]. As the horizontal resolution increases, the vortex structure becomes more compact, the maximum wind radius decreases, and then the outward inclination of maximum wind radius with height decreases as well.

The radius-height cross-section of vertical upward wind depicted in Fig.10 clearly shows the influence of horizontal resolution on the strength and structure of Rammasun updraft motion. As the horizontal resolution increases, the stronger updraft motion is concentrated in a narrower and deeper region. When the horizontal resolution increases from 15 km to 9 km and further to 3 km, the maximum vertical upward wind increases from below 1.75 m/s to more than 2.25 m/s and then to above 3.5 m/s, the radial width of the region with the vertical upward wind greater than 1.5 m/s decreases from approximately 30 km to approximately 26 km and then to approximately 18 km, and the height covered by this region increases from 200-500 hPa to 170-750 hPa and then to 150-850 hPa.

We have seen in Fig.6 that, at 48h, the eye wall of Rammasun is inclined outward with height, and the inclination decreases as the horizontal resolution increases. From the time-averaged results in Fig.10, we can further clearly see the difference of the eye wall structure with different horizontal resolution. The higher the horizontal resolution, the smaller the thickness of eye wall, and the stronger the updraft motion, and also the smaller the outward inclination of eye wall with height. For 3 km horizontal resolution, the outward inclination of eye wall mainly appears at the low levels below 700 hPa and the high levels above 300 hPa, while the inclination of the mid-level eye wall is almost zero. By comparing Fig.10 with Fig.9, we can see that

the vertical structure of eye wall is completely consistent with the vertical structure of tangential wind.

The radius-height cross-section of equivalent potential temperature depicted in Fig.11 shows the influence of horizontal resolution on the vertical thermodynamic structure of Rammasun. We can see from Fig.11 that regardless of whether the horizontal resolution is high or low, the distribution of equivalent potential temperature has the typical features of the distribution of TC equivalent potential temperature, which is consistent with the observations (Hawkins and Imbembo [20]). That is, the region with high equivalent potential temperature is located at the low and high levels of the eye region, while in its middle levels, the equivalent potential temperature is relatively low, and the equivalent potential temperature in the eye wall region is higher than that in its adjacent regions. When the horizontal resolution increases, as the eye region decreases and the thickness of eye wall narrows, the difference between the equivalent potential temperature in the eye wall region and in its adjacent regions increases, and when the horizontal resolution increases from 9 km to 3 km, the increase of the difference is more obvious in 500-800 hPa.

The updraft motion along the eye wall transports the moist and hot air mass from the boundary layer to high levels, making the equivalent potential temperature in the eye wall region higher than that of its adjacent regions. As the horizontal resolution increases, the updraft motion strengthens (Fig.10), and the strengthened updraft motion transports more moist and hot air mass, which makes the convective activity in the eye wall region stronger, and then the equivalent potential temperature in the eye wall region also becomes higher.

The radius-height cross-section of potential vorticity shown in Fig.12 further illustrates the influence of horizontal resolution on the vertical dynamic and thermodynamic structure of Rammasun. We can see from Fig.12 that for the horizontal resolution of 15, 9, or 3 km, the largest potential vorticity is located in 400-500 hPa, and for the horizontal resolution of 9 km and 3 km, the potential vorticity in the eye wall region is larger than that in its adjacent regions. When the horizontal resolution increases, both the largest potential vorticity and the radial gradient of potential vorticity increase. When the horizontal resolution increases from 9 km to 3 km, the increase is particularly obvious, and the largest potential vorticity increases from less than 30PVU to near 60PVU. As the horizontal resolution increases, the radial width of the region with potential vorticity greater than 3PVU decreases, which again shows the change of vortex structure from being loose to being compact.

The vertical structure of Rammasun with different horizontal resolution, as shown in Fig.12, is consistent with the results shown in Figs.9, 10, and 11. The strong wet convective activity in the eye wall region makes the potential vorticity in this region higher than that in its adjacent regions, and the increase of horizontal resolution further strengthens the convective activity in the eye wall region, which makes the potential vorticity in this region higher. In particular, when the horizontal resolution increases to 3 km, the enhancement of convective activity is more significant, so the increase of the largest potential vorticity is also more obvious. In addition, Fig.12 again indicates the characteristic that the outward inclination of eye wall with height decreases as the horizontal resolution increases.

The vertical wind shear has long been recognized to have strong effect on TC intensity. Here, we also compare the vertical wind shear of Rammasun simulated with three horizontal resolutions. Fig.13 shows the evolution of 850-200 hPa area-averaged vertical wind shear magnitude for a 600-km radius around the center of Rammasun simulated with three horizontal resolutions. From the figure, we can see that after about 10h, the vertical wind shear with different horizontal resolution shows obvious difference. The vertical wind shear decreases with the increase of horizontal resolution. The vertical wind shear with 3 km horizontal resolution is much smaller than that of 9 km, and the vertical wind shear with 9 km horizontal resolution is smaller than that of 15 km on the whole. However, although the vertical wind shears with three horizontal resolutions are different, their variation trends with time are basically the same. Their overall variation trends are all decreasing with time.

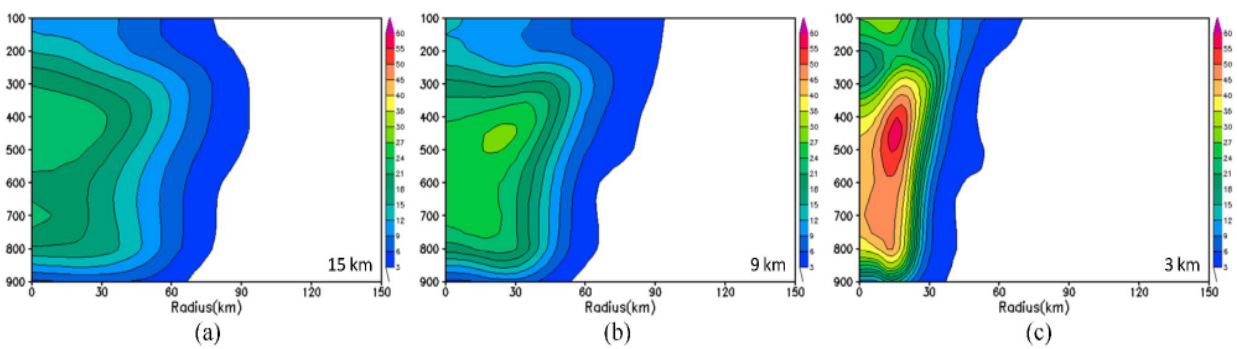

Figure 12. Axisymmetric 12-hourly (02:00-14:00 BJT, July 18) time-averaged radius-height cross-section of potential vorticity of Rammasun simulated with three horizontal resolutions (unit: PUV; a: 15 km, b: 9 km, c: 3 km).

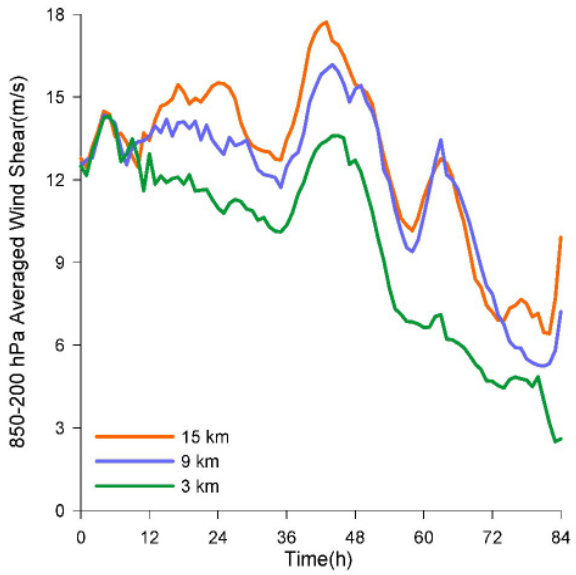

Figure 13. Temporal evolution of 850-200 hPa area-averaged vertical wind shear magnitude (from 08:00 BJT on July 16 to 20:00 BJT on July 19) for a 600-km radius around the center of Rammasun simulated with three horizontal resolutions (orange: 15 km, blue: 9 km, green: 3 km).

Generally, the larger the vertical wind shear, the weaker the TC intensity. The results of Fig.13 show that as the horizontal resolution increases from 15 km to 9 km and then to 3 km, the vertical wind shear reduces gradually, and corresponding to this, the Rammasun intensity increases gradually (Fig.2). Especially when the horizontal resolution increases from 9 km to 3 km, the vertical wind shear reduces significantly, and corresponding to this, the Rammasun intensity strengthens significantly (Fig.2). From the results of Fig. 13, we can further understand the difference among the Rammasun intensity simulated with three horizontal resolutions.

4.5 *Results of no method of convection parameterization*

In this section, we give the simulation results with the horizontal resolution of 9 km and 3 km when we do not adopt the method of convection parameterization for the model inner domain. Figs. 14 and 15, respectively corresponding to Fig.3b and 3c and Fig.8, show the evolution of axisymmetric tangential wind at 10m-height with time (Fig.14) and the evolution of axisymmetric maximum temperature anomaly with time (Fig.15) for Rammasun simulated with two horizontal resolutions when the method of convection parameterization is not adopted for the inner domain.

By analyzing the results in Fig.14 and comparing them with the results in Fig.3b and 3c, we find that the evolution process of Rammasun vortex with the two horizontal resolutions is similar, and it is consistent with the evolution process simulated using the KF scheme for the inner domain. However, there is difference between the intensity and scale of Rammasun vortex when the method of convection parameterization is not adopted and those when the KF scheme is adopted. When the method of convection parameterization is not adopted, the vortex intensity is weaker than the intensity when the KF scheme is adopted, and the vortex horizontal scale is smaller than the scale when the KF scheme is adopted. This difference is not considerable for 3 km horizontal resolution, but it is obvious for 9 km horizontal resolution, which makes the difference of the simulated vortex between the 9 km and 3 km horizontal resolution larger when the method of convection parameterization is not adopted than the difference when the KF scheme is adopted, especially the difference of vortex intensity.

The results in Fig.15 are similar to the results in Fig.14. From Fig.15, we can see that the difference between the strength of Rammasun warm core simulated with 9 km and 3 km horizontal resolution gradually increases after 21 h. The largest difference of axisymmetric maximum temperature anomaly reaches approximately 4.5K, which is much greater than the largest difference by approximately 2K when the KF scheme is adopted (Fig.8). The variation trend of warm core and the difference of warm core strength simulated with different horizontal resolution, shown in Fig.15, are completely consistent with the results of Rammasun intensity with different horizontal resolution, shown in Fig.2.

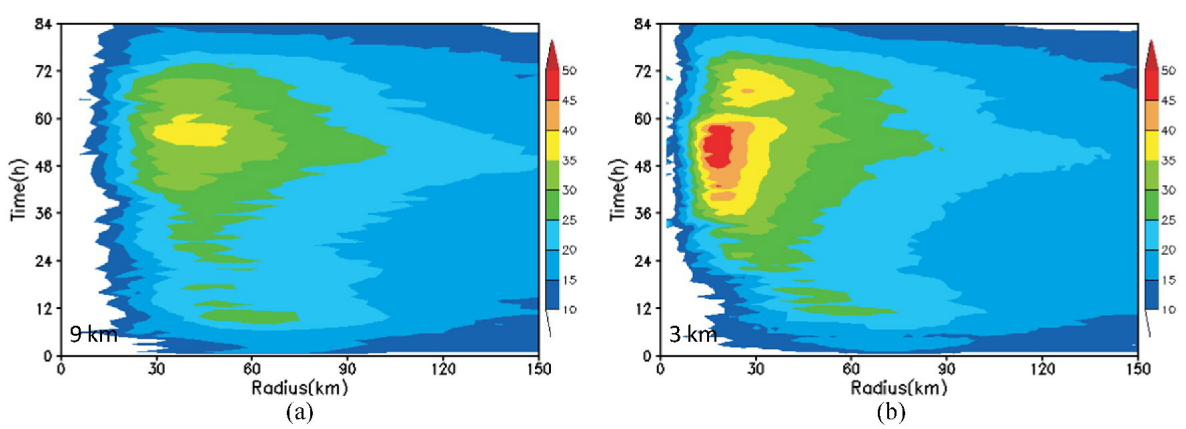

Figure 14. Temporal evolution of axisymmetric tangential wind at 10m-height (from 08:00 BJT on July 16 to 20:00 BJT on July 19) for Rammasun simulated with two horizontal resolutions (unit: m/s; a: 9 km, b: 3 km).

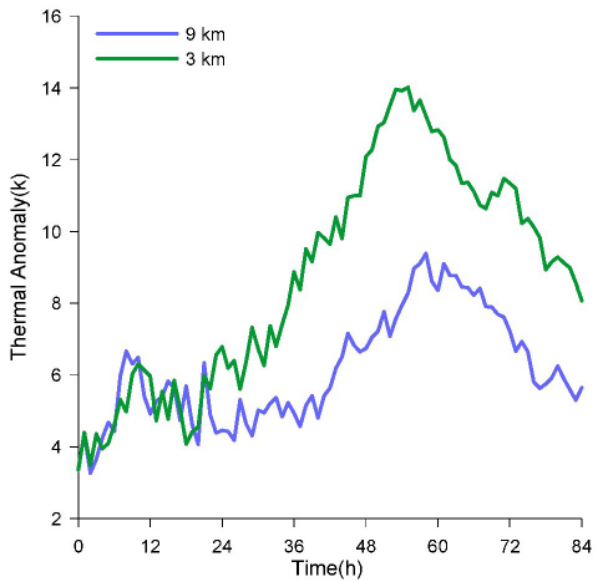

Figure 15. Temporal evolution of axisymmetric maximum temperature anomaly (from 08:00 BJT on July 16 to 20:00 BJT on July 19) for Rammasun simulated with two horizontal resolutions (blue: 9 km, green: 3 km).

Figures 14 and 15 and other results (figures not shown) all clearly indicate that when the method of convection parameterization is not adopted for the model inner domain, the change of Rammasun intensity and structure caused by the change of horizontal resolution is similar to the change when the KF scheme is adopted. The difference is that when the method of convection parameterization is not adopted, the change is clearly larger than the change when the KF scheme is adopted, because when the method of convection parameterization is not adopted, the Rammasun intensity simulated with 9 km horizontal resolution is much weaker than the intensity when the KF scheme is adopted. Therefore, for the simulation of Rammasun, when the horizontal resolution is 9 km, the model still needs to utilize the parameterization method to describe the convective process. When the horizontal resolution reaches 3 km, the model can describe the convective process without using the method of convection parameterization.

5 CONCLUSIONS AND DISCUSSION

In this paper, we use the WRF (V3.4) model as the experimental model and select three horizontal resolutions of 15, 9, and 3 km to make experiments on the super-strong typhoon Rammasun to research the influence of model horizontal resolution on the intensity and structure of Rammasun. The results are as follows:

(1) On the whole, the horizontal resolution has very little influence on the Rammasun track. The simulated tracks with the three horizontal resolutions are all very close to the observed track. In particular, the track with 9 km horizontal resolution is closest to the observed. The Rammasun intensity is highly sensitive to the change of horizontal resolution. The simulated intensity increases as the horizontal resolution increases. When the horizontal resolution increases from 9 km to 3 km, the enhancement of intensity is more obvious, but the strongest intensity simulated with 3 km horizontal resolution is still weaker than the observed.

(2) The Rammasun structure is also highly sensitive to the change of horizontal resolution. As the horizontal resolution increases, the horizontal scale of vortex decreases, and both the thickness of eye wall and the maximum wind radius decrease, and the wind in the inner core region increases. The strong wind region extends vertically to higher altitude, and the vortex is more compact and deeper. The updraft motion strengthens and concentrates in a narrower and deeper region, and the outward inclination with height of the maximum wind radius and eye wall decreases. The warm region located at the middle and high levels becomes narrow, and the warm core strengthens. The difference between the humidity in the eye wall region and that of the eye region increases, and the difference between the equivalent potential temperature in eye wall region and that of its adjacent regions also increases. In addition, the vertical wind shear reduces. This change is much greater when the horizontal resolution increases from 9 km to 3 km than the change when the horizontal resolution increases from 15 km to 9 km.

(3) When the method of convection parameterization is not adopted for the model inner region, the Rammasun intensity simulated with 3 km horizontal resolution is slightly weaker than the intensity with 3 km horizontal resolution when the KF convection scheme is adopted, and the simulated intensity with 9 km horizontal resolution is far weaker than the intensity with 9 km horizontal resolution when the KF scheme is adopted. When the method of convection parameterization is not adopted, the change of Rammasun intensity and structure caused by the change of horizontal resolution is clearly larger than the change when the KF scheme is adopted.

The model horizontal resolution has very little influence on the Rammasun track. This is because the Rammasun is in a strong environmental field and its movement is mainly controlled by the environmental guiding airflow. At present, most models are well able to forecast the large-scale environmental airflow. The level of horizontal resolution has very little effect on the forecasting of large-scale environmental field. So it can be seem from Fig.1 that the simulated Rammasun tracks with the three horizontal resolutions are very close.

However, the model horizontal resolution has great influence on the Rammasun intensity and structure. As the horizontal resolution increases, the vortex gradually contracts toward its center, and the vortex structure changes from being loose to being compact and deep. Both the thickness of eye wall and the outward inclination of eye wall with height decrease. The updraft

motion along the eye wall strengthens, transporting more moist and hot air mass from the boundary layer to high levels, which enhances the convective activity in the eye wall region and then enhances the strength of warm core. As the thickness of eye wall decreases, the pressure gradient force in the eye wall region increases, causing the wind in the eye wall region to increase. As the warm core strengthens and the thickness of eye wall decreases, the temperature gradient in the eye wall region also increases, which enhances the vortex circulation. The intensification of updraft motion causes the surface pressure to decline more, and then the surface wind becomes stronger. In addition, as the horizontal resolution increases, the vertical wind shear reduces. All of these factors make the Rammasun intensity stronger.

The increase of horizontal resolution increases the simulated intensity of Rammasun. However, when the horizontal resolution increases from 15 km to 9 km, the intensity enhances only slightly. When the horizontal resolution increases from 9 km to 3 km , the enhancement of intensity is relatively obvious. Nonetheless, the strongest intensity simulated with 3 km horizontal resolution is still weaker than the observed strongest intensity. Therefore, for the prediction and simulation of TC intensity, the model horizontal resolution needs to reach at least 3 km to obtain the results that are relatively close to the observations, which is consistent with the current understanding regarding the TC intensity forecasting (Rogers[11] ; Nguyen et al.[12]; Montgomery et al.[13]; Smith et al.[14]; Smith et al.[15]). From the simulation results when the method of convection parameterization is not adopted for the model inner domain, we can see that for the simulation of TC with vigorous convective activity, only when the horizontal resolution reaches 3 km, can it be possible for the model not to use the method of convection parameterization.

In this paper, we make experiments to research the influence of horizontal resolution on TC intensity and structure, but the experiments are only for Rammasun. So the obtained conclusions are only for Rammasun. To obtain universal conclusions, we need to make more experiments for more TCs. For Rammasun, is it possible to get the simulation result of intensity closer to the observation by other ways, such as improving the schemes of some physical processes in the model? To answer this question, we need to make further experiments.

REFERENCES:

[1] DUAN Yi-hong, CHEN Lian-shou, XU Ying-long, et al. The status and suggestions of the improvement in the typhoon observation, forecasting and warning systems in China [J]. Engineering Sci, 2012, 14(9): 4-9 (in Chinese).

[2] XU Ying-long, ZHANG Ling, GAO Shuan-zhu. The advances and discussions on China operational typhoon forecasting [J]. Meteor Mon, 2010, 36 (7): 43-49 (in Chinese).

[3] QIAN Chuan-hai, DUAN Yi-hong, MA Su-hong, et al. The current status and future development of China operational typhoon forecasting and its key technologies [J]. Adv Meteor Sci Tech, 2012, 2(5): 36-43 (in Chinese).

[4] CANGIALOSI J P, FRANKLIN J L. 2011 National Hurricane Center verification report [C]. Tropical Prediction Center, National Hurricane Center, National Center for Environmental Prediction, National Weather Center, NOAA, 2012: 76 pp.

[5] HILL K A, LACKMANN G M. Analysis of idealized tropical cyclone simulations using the Weather Research and Forecasting Model: Sensitivity to turbulence parameterization and grid spacing [J]. Mon Wea Rev, 2009, 137(2): 745-765.

[6] GOPALAKRISHNAN S G, JR F M, ZHANG X, et al. The experimental HWRF system: A study on the influence of horizontal resolution on the structure and intensity changes in tropical cyclones using an idealized framework [J]. Mon Wea Rev, 2011, 139(6): 1762-1784.

[7] BRAUN S A, TAO W K. Sensitivity of high-resolution simulations of Hurricane Bob (1991) to planetary boundary layer parameterizations [J]. Mon Wea Rev, 2000, 128(12): 3941-3961.

[8] GENTRY M S, LACKMANN G M. Sensitivity of simulated tropical cyclone structure and intensity to horizontal resolution [J]. Mon Wea Rev, 2010, 138 (3): 688-704.

[9] DAVIS C, WANG W, DUDHIA J, et al. Does increased horizontal resolution improve hurricane wind forecasts? [J]. Wea Forecasting, 2010, 25(6): 1826-1841.

[10] DAVIS C, BOSART L F. Numerical simulations of the genesis of Hurricane Diana (1984). Part II: Sensitivity of track and intensity prediction [J]. Mon Wea Rev, 2002, 130(5): 1100-1124.

[11] ROGERS R. Convective-scale structure and evolution during a high-resolving simulation of tropical cyclone rapid intensification [J]. J Atmos Sci, 2010, 67(1): 44-70.

[12] NGUYEN V S, SMITH R K, MONTGOMERY M T. Tropical cyclone intensification and predictability in three dimensions [J]. Quart J Roy Meteor Soc, 2008, 134(632): 563-582.

[13] MONTGOMERY M T, NGUYEN V S, PERSING J, et al. Do tropical cyclones intensify by WISHE? [J]. Quart J Roy Meteor Soc, 2009, 135(644): 1697-1714.

[14] SMITH R K, MONTGOMERY M T, VOGL S. A critique of Emanuel's hurricane model and potential intensity theory [J]. Quart J Roy Meteor Soc, 2008, 134 (632): 551-561.

[15] SMITH R K, MONTGOMERY M T, SANG N V. Tropical cyclone spin-up revisited [J]. Quart J Roy Meteor Soc, 2009, 135(642): 1321-1335.

[16] YING M, ZHANG W, YU H, et al. An overview of the China Meteorological Administration tropical cyclone database [J]. J Atmos Oceanic Technol, 2014, 31 (2): 287-301.

[17] YAU M K, LIU Y, ZHANG D L, et al. A multiscale numerical study of Hurricane Andrew (1992). Part VI: Smallscale inner-core structures and wind streaks [J]. Mon Wea Rev, 2004, 132(6): 1410-1433.

[18] DAVIS C, COAUTHORS. Prediction of landfalling

hurricanes with the Advanced WRF model [J]. Mon Wea Rev, 2008, 136(6): 1990-2005.

[19] STERN D P, NOLAN D S. Reexaming the vertical structure of tangential winds in tropical cyclones: Observation and theory [J]. J Atmos Sci, 2009, 66(12): 3579-3600.

[20] HAWKINS H F, IMBEMBO S M. The structure of a small, intense hurricane, Inez (1966) [J]. Mon Wea Rev, 1976, 104(4): 418-442.

Citation: WANG Chen-xi and ZENG Zhi-hua. Influence of model horizontal resolution on the intensity and structure of Rammasun [J]. J Trop Meteor, 2018, 24(1): 15-28.